Physica B 535 (2018) 44–49

Contents lists available at ScienceDirect

Physica B

journal homepage: www.elsevier.com/locate/physb

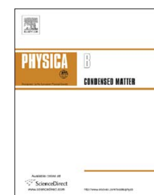

Defects in silicon carbide grown by fluorinated chemical vapor deposition chemistry

Pontus Stenberg, Ian D. Booker, Robin Karhu, Henrik Pedersen, Erik Janzén, Ivan G. Ivanov*

Department of Physics, Chemistry and Biology, Linköping University, 581 83 Linköping, Sweden

A R T I C L E I N F O

Keywords:
Fluorinated chemical vapor deposition
Defects
Photoluminescence
Deep-level transient spectroscopy

A B S T R A C T

Point defects in *n*- and *p*-type 4H-SiC grown by fluorinated chemical vapor deposition (CVD) have been characterized optically by photoluminescence (PL) and electrically by deep-level transient spectroscopy (DLTS) and minority carrier transient spectroscopy (MCTS). The results are considered in comparison with defects observed in non-fluorinated CVD growth (e.g., using SiH_4 instead of SiF_4 as silicon precursor), in order to investigate whether specific fluorine-related defects form during the fluorinated CVD growth, which might prohibit the use of fluorinated chemistry for device-manufacturing purposes. Several new peaks identifying new defects appear in the PL of fluorinated-grown samples, which are not commonly observed neither in other halogenated chemistries, nor in the standard CVD chemistry using silane (SiH_4). However, further investigation is needed in order to determine their origin and whether they are related to incorporation of F in the SiC lattice, or not. The electric characterization does not find any new electrically-active defects that can be related to F incorporation. Thus, we find no point defects prohibiting the use of fluorinated chemistry for device-making purposes.

1. Introduction

4H-SiC is a wide indirect bandgap semiconductor of interest for electronic power devices such as unipolar MOSFETs or insulated gate bipolar transistors (IGBTs) [1]. In these and other applications, the chemical vapor deposition (CVD) is the most common technique to grow the material for the active layers. Apart from the traditional CVD growth of SiC using ethylene (C_2H_4) and silane (SiH_4) as carbon and silicon precursors, respectively, the use of chlorine in a SiC CVD process has been found beneficial since chlorine binds stronger to Si than Si to another Si (Si-Cl binding energy is 417 kJ/mol compared to Si-Si, 310 kJ/mol [2]). Therefore, the presence of Cl inhibits the homogenous nucleation of Si in the gas phase and strongly reduces the probability of formation of Si droplets during growth. Also, high growth rates exceeding 100 μm/hour have been demonstrated with chlorinated CVD growth [3]. Fluorine is another halogen which forms even stronger than Cl bond to Si (Si-F binding energy is 576 kJ/mol [2]). Therefore, the fluorinated chemistry is expected to provide advantages similar to the chlorinated one. Due to its high electronegativity, F forms also strong bonds to other elements (e.g., F-Br, F-Ti). This circumstance can potentially alter the unintentional incorporation of foreign elements in the SiC lattice by binding them to F in the gas phase, before they are incorporated into the epitaxial layer. Due to the strong bonding, however, F itself can be adsorbed on the surface via fluorinated growth species and potentially incorporate into the growing layer [4]. Considering the chlorinated growth, it has been shown by means of secondary-ion mass spectrometry (SIMS) that Cl incorporates into the grown epilayers in concentration of $\sim 1\times10^{14}$ cm^{-3}. This is however uncertain since the measured value is close to the detection limit [5]. Following this finding, several publications have investigated the possibility of appearance of Cl-related defects or defect complexes in the epitaxial layers [6–9]. However, while ab initio calculations have predicted several defect configurations, such as $Cl_C - V_{Si}$ complexes, Cl_i interstitials or Cl_C substitutional defects to be possible, none of these defects has ever been clearly demonstrated experimentally [9].

The incorporation of F and other atomic species in SiC grown using fluorinated chemistry has not been studied so far. Intrinsic defects specific to the growth chemistry also may form during growth. Some of the intrinsic and extrinsic defects may be electrically active and have undesired influence on the device performance, because they may trap charge carriers or provide unwanted recombination channels. Therefore, it is necessary to analyze and understand which point defects are present in the as-grown epitaxial layers. In all chemistries, the defect formation is influenced by the various growth parameters. Thus, tuning the parameters may be used as a means of controlling the

* Corresponding author.
E-mail address: ivani@ifm.liu.se (I.G. Ivanov).

http://dx.doi.org/10.1016/j.physb.2017.06.030
Received 17 April 2017; Received in revised form 11 June 2017; Accepted 12 June 2017
Available online 13 June 2017
0921-4526/ © 2017 Elsevier B.V. All rights reserved.

formation of undesired defects, at least to some extent.

As a first step towards better understanding of the defect formation in fluorinated CVD growth, in this work we investigate the photoluminescence (PL) and deep level transient spectroscopy (DLTS) of the samples grown under different conditions using fluorinated chemistry. Both n- and p-type samples are investigated from point of view of possibility to dope (n- and p-type) during fluorinated growth, as well as formation of intrinsic and extrinsic defects in the epitaxial layers. The results are considered in comparison with those obtained from epitaxial layers grown by other chemistries.

2. Methods

2.1. Growth

A horizontal hot wall chemical vapor deposition system was used for the growth of both n- and p-type doped SiC epitaxial layers. The growth chamber was a graphite susceptor coated with SiC. No rotation of the substrates was available using this susceptor. The growth was performed on substrates of size 16 mm×16 mm. Standard 4H-SiC substrates with 4° off-cut angle towards $[11\bar{2}0]$ were used, with a constant position in the susceptor during growth.

CH_4 and SiF_4 were used as C and Si precursors, respectively. The latter was also the source of F in the growth chamber. The n- and p-type doping was implemented using during growth controlled flow of N_2 and trimethylaluminum (TMAl) for N (*n*-type) and Al (*p*-type) doping, respectively. H_2 purified using palladium membrane was used as carrier gas. The concentration of SiF_4 in H_2 was 0.125%, thus Si/H_2 = 0.125%. The samples were grown at process temperature of 1600 °C and process pressure of 100 mbar with the samples positioned ~6 cm inside the susceptor.

The dopant precursor concentrations were varied in the range 0.1–10 for the N_2/Si ratio and 10^{-5} to 10^{-2} for the Al/Si ratio using C/Si = 1. Also, one additional experiment using N_2/Si = 100 was performed. In this latter experiment the amount of H_2 carrier gas was reduced to compensate for the high flow of N_2. This resulted in Si/H_2 = 0.144% (instead of Si/H_2 = 0.125%). However, the C/Si ratio and the process pressure and temperature were maintained the same as for the rest of the runs.

The C/Si ratio was varied in the range 0.4–1.2 in steps of 0.2, while the dopant-to-silicon ratios were N_2/Si = 1 for N-doped samples and Al/Si = 10^{-4} for Al-doped samples.

The growth time for the nitrogen doped (*n*-type) samples were 0.5 h and 2.0 h for the aluminum doped (*p*-type) samples. This resulted in thicknesses of the epitaxial layers between 4 and 5 μm for the n-type samples, and about 16–20 μm for the p-type samples. The growth rate increases with the C/Si ratio approximately linearly from 8 μm/hour at C/Si = 0.4–10 μm/hour at C/Si = 1.2.

Growth of thicker layers was also attempted. One additional sample grown at temperature of 1650 °C, pressure 100 mbar, Si/H_2 = 0.25% and C/Si = 0.5. In this case, ethylene (C_2H_4) was used as carbon precursor. The sample was grown for 5 h using N_2 as a dopant with ratio of N_2/Si=0.15. This particular sample has a thickness of ~100 μm.

2.2. Photoluminescence (PL)

The photoluminescence of the samples was measured using 244 nm excitation from a frequency-doubled Ar ion laser. The detection part consists of a Jobin-Yvon monochromator (HR460) equipped with a grating of 2400 g/mm and a CCD camera. This results in a spectral resolution of ~0.5 Å (full width at half maximum, FWHM). The samples were kept in a He bath cryostat at a temperature of 2 K.

2.3. Deep level transient spectroscopy (DLTS) and Minority Carrier Transient Spectroscopy (MCTS)

Schottky contacts of 1.2 mm diameter are deposited by thermal evaporation of Ni (100 nm thickness). Silver paste on the highly conductive substrate provided the Ohmic contacts. The capacitance transients were measured in the temperature range 77–600 K, using a reverse bias of −10 V and a superimposed 10 V filling pulse (up to a total of 0 V) of 1 ms to 10 ms duration. GS4 correlation function was used to calculate the spectra. [10].

3. Results and discussion

We consider first the doping experiments which aim at obtaining 4H-SiC epilayers of n- and p-type with different controllable doping concentrations. The donor and acceptor doping concentrations of the various samples are assessed by C-V measurements, which indicate that in both cases (donors / acceptors) the doping concentration is approximately proportional to the corresponding gas flow of the dopant carrier (N_2 for n-type doping, and TMAl for p-type). For N-doped uncompensated samples (with negligible acceptor concentration), and if the donor doping concentration is below ~2×10^{16} cm^{-3}, the concentration can be estimated also from the PL spectra [11].

3.1. Photoluminescence

Let us consider now the low-temperature photoluminescence spectra of the n-type samples (nitrogen-doped). Fig. 1(a) shows the PL spectra in the near-band gap region of the samples N-doped to different concentrations, grown with C/Si=1.0. The spectra exhibit the usual no-phonon lines of the nitrogen-bound exciton (N-BE) denoted by P_0 and Q_0, as well as the phonon replicas P_{xx} (mainly of the P_0 line). In addition, the prominent phonon replicas of the free-exciton emission, whenever observable, are denoted with the symbols I_{xx}. In both cases of free- and bound-exciton replicas, the subscript 'xx' denotes the approximate phonon energy (in meV) of the phonon involved in the phonon-assisted recombination [12]. The appearance of two no-phonon lines for the N-BE instead of one is due to the existence of two inequivalent lattice sites within the 4H-SiC unit cell. Therefore, N donors occupying the one or the other inequivalent carbon site have quite different properties, in particular, different ionization energies and exciton binding energies, giving rise to two distinct no-phonon lines in the PL spectrum [13]. On the other hand, the ionization energy of the N donor at the so-called hexagonal lattice site (the other inequivalent one is called "cubic") has approximately two times lower ionization energy than the N donor at cubic site [13], which leads to ~2 times lower exciton binding energy for the former one, in accord with Haynes rule [14]. Therefore, the N-bound exciton at the hexagonal site, which is much more similar to the free exciton than the N-bound exciton at cubic site, exhibits weak no-phonon line (the free-exciton no-phonon line is forbidden by moment conservation law in indirect semiconductors) and strong phonon replicas (which are the only allowed radiative recombination paths if free-exciton recombination is considered). Thus, the N-BE at hexagonal site is responsible for the appearance of the weaker no-phonon P_0 line in the spectra and its significantly stronger phonon replicas. Conversely, the more strongly bound N-BE at cubic site is responsible for the appearance of the substantially stronger no-phonon Q_0 line, but its phonon replicas are negligible.

For the lowest-doped samples (the two bottom curves in Fig. 1(a)) the free-exciton replica I_{76}, which is strongest in intensity, can be recognized and used for estimation of the N-doping concentration by the method of Ref. [11]. Thus, for the sample with N_2/Si = 0.1 we obtain N-donor concentration [N] = 4×10^{14} cm^{-3}, whereas for the sample with N_2/Si = 1 we estimate [N] ≈ 8×10^{15} cm^{-3}. These values are in excellent agreement with the values of $N_D–N_A$=4×10^{14} cm^{-3} and

Download English Version:

https://daneshyari.com/en/article/8161032

Download Persian Version:

https://daneshyari.com/article/8161032

Daneshyari.com